Building Simulation

Seventh International IBPSA Conference
Rio de Janeiro, Brazil
August 13-15, 2001

NEW FAÇADE SYSTEM CONSISTING OF COMBINED PHOTOVOLTAIC AND SOLAR THERMAL GENERATORS WITH BUILDING INSULATION

Stefan Krauter, Mohammed J. Salhi, Sandra Schroer, Rolf Hanitsch
UFRJ-COPPE-EE, Caixa Postal 68504, Rio de Janeiro, 21945-970 RJ, Brazil
SOLON AG für Solartechnik, Schlesische Str. 27, D-10997 Berlin, Germany
Berlin University of Technology, Sec. EM 4, Einsteinufer 11, 10587 Berlin, Germany

ABSTRACT

Most photovoltaic (PV) facades are built as curtain facades in front of thermally insulated buildings with air ducts in between. This causes additional costs for support structure and installation, while heat dissipation from the solar cells is often not optimal. Measurements carried out are facing both concerns: Integration of a thermal insulating layer (which meets the latest German heat preserving regulation WSV 95) into the PV facade plus additional cooling by active ventilation or water flow. Simulation of different system configurations by an energy flow balance model were compared to actual measurements and showed relative small deviations. Active ventilation at conventional curtain PV facades allows a reduction of cell operating temperatures of 18 K, resulting in an 8% increase in electrical energy output at an air velocity of about 2 m/s. Cell temperatures increase by 20.7 K at thermal insulating PV facade elements (TIPVE) without cooling, which causes a 9.3% loss of electrical yield, but installation costs can be reduced by 20% (all related to a conventional PV curtain plus a heat insulating facade at a building). HYTIPVE, a hybrid thermal insulating PV facade element combined with a water-cooling system, which could also serve for hot water heating, lowers operating cell temperature by 20 K and increases electrical yield by 9% (referred to conventional curtain PV facades). Further economic investigations of such HYTIPVE including operational costs and substitution effect related to the yield are on the way.

INTRODUCTION

The application of solar energy technology in buildings often depends on its ability to be integrated into common building structures such as facade elements. Costs of planning, manufacturing and installation may be reduced if components as substrate, weather protection, photovoltaic (PV) generator, solar thermal collector, thermal insulation and mounting elements could be combined. Especially the thermal behavior of the PV generator has been investigated for different configurations of the facade structure.

Increased cell temperatures of PV modules lower the power output of typical crystalline silicon PV power plants by -0.3 %/K to -0.5 %/K (see Emery *et al*. 1996, Wilshaw *et al.* 1996). Therefore as electrical yield losses at high operating cell temperatures may be considerable, simulation and control of heat transfer is important. Although good heat transfer (passive or even active) is preferable, installation and mounting costs also have to be taken into consideration for PV facades. Four different kinds of PV facades – passively and actively cooled, also in combination with an integrated thermal insulation for the building – have been investigated. One part of the investigation (forced backside convection by fans) was carried out at a test facility of the "Laboratorio Fotovoltaico" at "Universidade Federal do Rio de Janeiro"; further testing took place at SOLON AG, Berlin. Earlier work predicts a reduction of cell operating temperature of 3-4 K only for passive cooling by natural convection on the backside of the facade. Other authors mention higher values (Hänel and Imamura 1992, Bloem and Ossenbrink 1995, Bendel *et al*. 1997, Brinkworth *et al.* 1997, Nordmann *et al.* 1997, Crick *et al*. 1997, Crick *et al*. 1998, Sandberg *et al.* 1998). For the most part literature reports on thermal performance of certain given facades, making it difficult to compare results. The following investigation has been undertaken to achieve more accurate results in a direct comparison of four very different thermal layouts under static conditions. This was carried out as a prerequisite for an economic evaluation of a new combined facade element that serves as a building insulation, generates electrical power at a high photovoltaic conversion efficiency and allows the use of solar thermal energy as well.

EXPERIMENT

2.1 Test conditions and equipment

The SOLON PV modules (1220 mm by 560 mm by 35 mm with frame) used in the studies consist of 36 multi-crystalline silicon solar cells (edge of 125 mm) and have an output power of 68 W under Standard Test Conditions (cell temperature of 25°C, irradiance of 1000 W m^{-2} and a solar spectrum equivalent to AM 1.5), see Table 1. The "artificial wall" to which the PV modules were mounted, for the experiments described, was made of smoothened pressboard (2 m wide, 2 m in height and 20 mm thick). The hall in

which the experiments were carried out was 32 m by 16 m with a height of 6 m and got a white plaster inner surface.

Table 1. Nominal Electrical Data of the PV modules used (at Standard Test Conditions)

Parameter	Solon PV module
Power at MPP (STC) P_{mpp}	68 W
Open circuit voltage V_{oc}	21.2 V
Short circuit current I_{sc}	4.42 A
Temperature coefficients TC_V, TC_C, TC_P	-77 mV/K, 1.5mA/K, -0.35 W/K
Maximum Power Point V_{mpp}, I_{mpp}	17.3 V, 3.93 A

The sun simulator was a "Steady-State-Simulator" using tungsten-halogen lamps of the type "HQI-T 2000W/D/I" by Osram, Berlin. The spectrum of the lamps and the AM 1.5 standard spectrum are plotted in Fig. 1

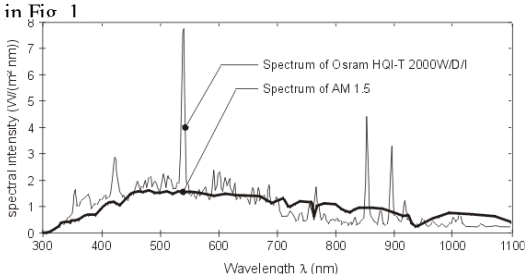

Figure 1. Spectrum of the solar simulator used in the experiments in comparison to AM 1.5.

Taking into account the decrease in average intensity due to the tilt angle of facades, an irradiance level of 700 W m^{-2} is adequate. The actual average irradiance achieved was 702 W m^{-2}, with a maximum at 749 W m^{-2} and a minimum of 655 W m^{-2}. Homogeneity of irradiance on the plane of the module was ± 6.7%. The PV facade elements were always operated at the maximum power point. Temperature measurements (ambient temperature, as well as upper and bottom back of the PV module temperatures) were made using Pt 100 temperature sensors at one-minute intervals until temperatures reached stationary values (see also Fig. 2 to Fig. 6).

2.2 Passively ventilated PV facade element

In the first experimental arrangement, representing a conventional PV curtain facade, a variable air duct was let between the facade and the wall. Figure 2 shows the test set-up of this passive ventilated PV facade.

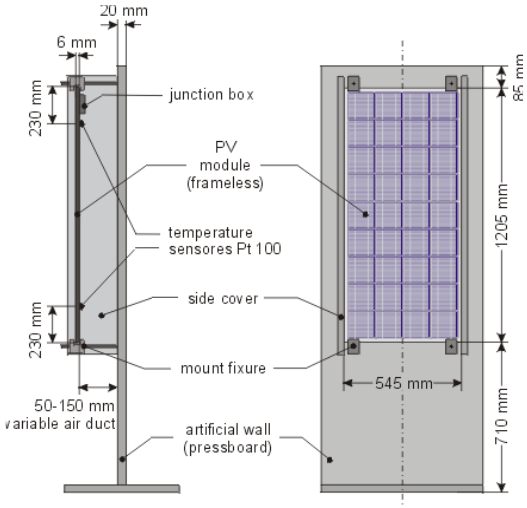

Figure 2. Side- and front view of the passively ventilated PV facade element (curtain facade).

The frame of the PV module was removed, to allow undisturbed natural convection in the air duct behind the module. The frameless module was 6 mm thick, 1205 mm long and 545 mm wide. To avoid disturbances of the convective airflow from the sides, a side cover was attached on both sides. Pt 100 temperature sensors were attached to the backside of the PV module 23 cm away from the edges and centered. Table 2 shows the stationary temperatures for t>30min (duration of measurements). Irradiance was 700 W m^{-2} on the plane of the facade by the solar simulator described above.

Table 2. Comparison of stationary temperatures at a passively ventilated PV facade element

Width of air duct (mm)	T_{cell} (°C)	$T_{upper} - T_{lower}$ (K)	T_a (°C)	ΔT_{cell} (K) *)
50	56.3	7.4	20.1	2.6
100	57.4	6.4	22.0	1.7
150	55.9	4.7	22.2	0

*) related to an air duct of 150 mm for T_a = 20°C (K)

While the effect of the variation of the air duct is 2.6 K only (see Table 2), it could be neglected in terms of output power in the observed range.

2.3 Actively ventilated PV facade element

The "Laboratorio Fotovoltaico" at "Universidade Federal do Rio de Janeiro (UFRJ) has carried out these measurements. In order to minimize the dispersion of air velocity along the width of the PV facade, an array of 16 fans was used. The aim of this experiment was to evaluate the maximum possible

effect of active ventilation: Therefore front- and backside of the PV module were both ventilated and the module was mounted with its long side towards horizontal (see Fig. 3.). The air velocities (measured at the front of the module, 40 mm above the module surface) shown in column A of Table 3 allowed a reduction of cell temperature by 16 K relative to natural convection. This resulted in an increase in power output by 7.2%.

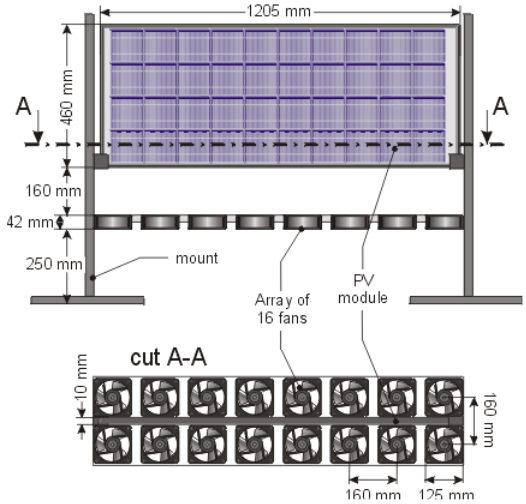

Figure 3. Side- and top view of the actively ventilated PV module.

Table 3. Distribution of forced convection air velocity v in m/s at the front of a PV facade element (average values measures 4 cm above module surface)

v (m/s)	Edge of PV facade		Center of PV facade	
Probe	A	B	A	B
Upper	0.95	1.65	1.35	2.1
Center	1.0	1.9	1.55	2.4
Lower	1.4	2.25	1.6	2.5

A further experiment (col. B, Table 3) was carried out with the same configuration, but an increased air velocity (about 50% more) that resulted in a reduction of 18 K in temperature and a power gain of 8.1% (both related to natural convection). Energy consumption of the fans was not measured. If active ventilation could be implemented inexpensively and with low power consumption, an appreciable decline in power generation costs would be possible.

2.4 Thermal insulating PV facade element TIPVE

Thermal insulation (12.5 cm layer of mineral wool) was attached directly to the backside of the PV facade in order to achieve a thermal insulation of 0.32 W K^{-1} m^{-2} in accordance with WSV 95 (Heat Preserving Regulation for Building Materials by the German Government 1995). This allows the substitution of the insulation layer of the building wall. Fig. 4 shows the test arrangement (temperature measurement configuration was the same as the one used at the conventional PV facade element, as shown in Fig. 5).

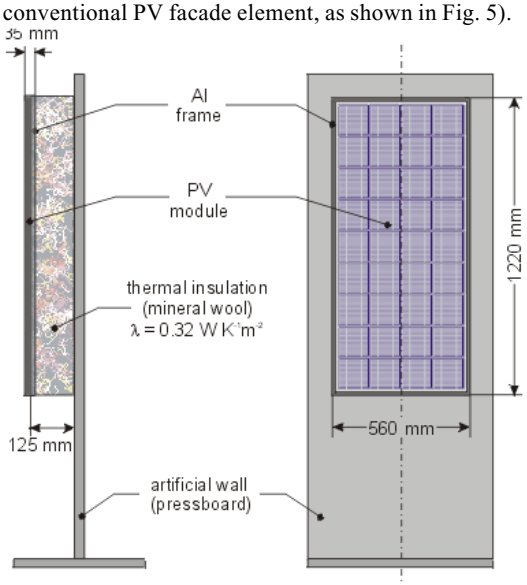

Figure 4. Side- and front view of the thermal insulating PV facade element (TIPVE).

As can be seen by rough comparison of Table 4 with Table 2, T_{center} at TIPVE is about 20 K higher than at a conventional PV facade element, which results in a 9% loss of electrical power output, while the TIPVE will lower the building equipment costs compared to a conventional arrangement including a thermal insulated wall plus a curtain PV facade with an air duct.

Table 4. Average values of cell- and ambient temperatures at thermally insulated PV facades

T_{upper}	T_{lower}	T_{upper}-T_{lower}	T_a	T_{center}
82.2 °C	72.1 °C	10.1 K	22.8 °C	77.2 °C

2.5 Hybrid thermal insulating PV facade (HYTIPVE)

The most recent development is a thermal insulating PV facade along with an integrated cooling system consisting of a propylene mat and a small water pump (see Fig. 5). The heated water could be used for thermal applications also (directly or combined with solar thermal systems). A model of such PV/thermal systems has been presented by Bergene and L□vvik 1995. Table 5 shows the measured stationary temperatures at different flow rates while using an inlet water temperature of 13.6°C to 15.8°C (water inlet temperature was constant during each experiment). HYTIPVE offers an additional cooling effect of about 20 K compared with conventional PV curtain facades, and is in the same range as active ventilated

structures (max. 18 K). The heat flow in the flowing water is about 380 W m^{-2}, see Table 8.

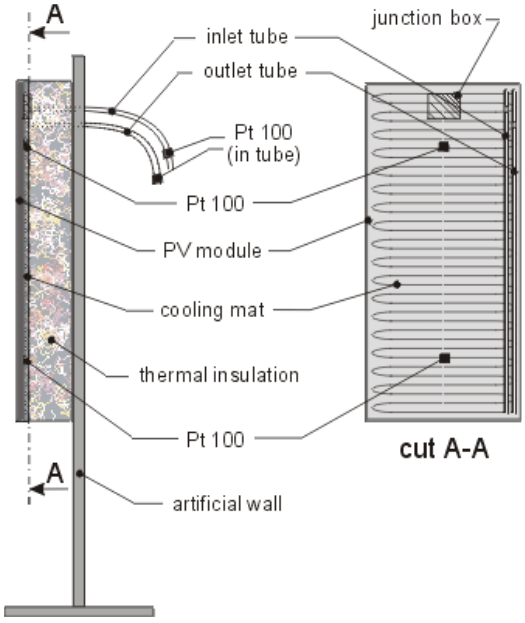

Figure 5. Side- and rear view of the hybrid thermal insulating PV facade element (HYTIPVE).

Table 5. Temperatures of a hybrid thermally insulated PV facade element (HYTIPVE)

	Flow rate in m^3/s		
	37· 10^{-6}	43· 10^{-6}	47.7· 10^{-6}
T_{cell} in °C	37.6	39.7	36.8
$T_{ambient}$ in °C	22.2	24.0	23.1
ΔT_{cell} in K *)	2.2	1.9	0
T_{inlet} in °C	13.6	15.8	12.6
T_{outlet} in °C	15.4	17.1	13.9

*) related to a flow rate of 47.7· 10^{-6} m^3/s (for T_a = 20°C)

SIMULATION OF ENERGY FLOWS

The theoretical background for the different energy flows at the experiments shown is presented below. The calculation of the heat fluxes was carried out, basing on the measured temperatures, and comparing the results to the actual measurements of irradiance. The total heat flow q generated by a PV facade element could be described by:

$$q = G \cdot (1 - \rho_{opt} - \eta_{PV}) \qquad (1)$$

Reflection losses ρ_{opt} depend on the optical properties of the materials, incidence angle and solar spectrum, while photovoltaic conversion efficiency η_{PV} is a function of irradiance, solar spectrum and operating temperature. A detailed model of the optical, thermal and electrical parameters defining reflection losses, heat flow, cell temperature and performance is given by Krauter 1993 and by Krauter and Hanitsch 1996. The reflection losses ρ_{opt} for the modules used (calculated with a three layer model, including optical dispersion and non-ideal antireflective coating) amount to 13.1%. The actual photovoltaic conversion efficiency η_{PV} measured at G = 700 W m^{-2} and T_{cell} = 27°C was 8.5% for a frameless PV module.

For equilibrium conditions the generated heat flow q has to be dissipated by conduction (q_k), convection (q_c) and radiation (q_r) from the front (subscript f) and back surface (subscript b) of the PV module. In the case of additional thermal use (HYTIPVE), the heat flow dissipation by the flowing water has to be considered also (q_w):

$$q = q_k + q_c + q_r + q_w \qquad (2)$$

$$q = q_{kf} + q_{kb} + q_{cf} + q_{cb} + q_{rf} + q_{rb} + q_w \qquad (3)$$

Due the type of mounting heat flow by conduction is negligible if no insulation material is used on the backside. At the experiments that do have a backside insulation heat dissipation by convection and by radiation on the back can be neglected. For the experiments with the curtain facade the radiation exchange between the module and the back wall is considered as a heat exchange between quasi-infinite parallel plates:

$$q_{rb} = \frac{\sigma\left(T_b^4 - T_{aw}^4\right)}{\frac{1}{\varepsilon_b} + \frac{1}{\varepsilon_{aw}} - 1} \qquad (4)$$

The emittances of the materials can be found in Table 7. Doing radiation calculations temperatures are to be expressed in Kelvin. Therefore no measurements could be taken from the artificial wall, the arithmetic average of back temperature and ambient temperature was used. Setting front and back temperature equal to cell temperature results in an error of 1.5 K only (Krauter 1993).

Therefore the floor temperature is the same as ambient temperature, the view factor is unity and the radiation exchange of the module front with the wall and the floor results in:

$$q_{rf} = \sigma \cdot \varepsilon_f \cdot (T_f^4 - T_{wall}^4) \qquad (5)$$

To simplify the calculations, wall temperature is set to ambient temperature.

Therefore the experiment with forced convection is set up symmetrically and was located relatively far away from the back wall q_{rb} can be calculated equivalently to (5) using T_b and ε_b. The heat flux generated by convection of air at the front surface of the module is:

$$q_{cf} = h_{cf} \cdot (T_f - T_a) \qquad (6)$$

For natural convection the heat transfer coefficient h_{cf} at a surface of a PV facade element with the length l

could be expressed by h_{nc} as follows (according to Merker 1987):

$$h_{nc} = \frac{k}{l} Nu_{nc} = 0.56 \frac{k}{l} Ra^{1/4} \qquad (7)$$

$$Ra = Pr \cdot Gr = Pr \cdot \frac{g \; l^3}{\nu^2} \left(T_f - T_a \right) \qquad (8)$$

The backside of the PV curtain facade could be modeled as an air-duct with heating from one side. For this case (Gr >1) VDI 1994 gives a solution as follows:

$$Nu = .61 \cdot \left(Pr \cdot Gr \right)^{1/4} = .61 \cdot \left(Pr \cdot \frac{g\beta (T_b - T_{aw}) d^4}{\nu^2 l} \right)^{1/4} \qquad (9)$$

The properties for air required could be found in Table 6 as a function of temperature. According to VDI 1994 a reasonable value to use as reference temperature for these properties is the average between ambient and body temperature. Sandberg and Moshfegh (1998) have carried out further investigations on this subject.

For forced convection within a range of $.13 \cdot 10^{-3}$ m s^{-1} < v < $1.33 \cdot 10^{2}$ m s^{-1} the heat transfer coefficient can be found (derived from VDI 1994 and Merker 1987) as:

$$h_v = \frac{k \, Nu_v}{l} = \frac{k}{l} \left(Nu_{lam}^2 + Nu_{tur}^2 \right)^{1/2} \qquad (10)$$

$$Nu_{lam} = 0.664 \cdot \mathrm{Re}^{1/2} \, Pr^{1/3} \qquad (11)$$

$$Nu_{tur} = \frac{0.037 Pr \, \mathrm{Re}^{0.8}}{1 + 2.433 \mathrm{Re}^{-0.1} \left(Pr^{2/3} - 1 \right)} \qquad (12)$$

with:

$$Re = \frac{v \rho l}{\mu} \qquad (13)$$

At the experiment for forced convection, front and back heat transfer is about the same:

$$q_{cb} \approx q_{cf} = h_v (T_f - T_a).$$

For air velocities v < 1 m s^{-1} heat transfer by natural convection could be more than by forced convection. In case of similar direction of natural and forced convection Churchill 1977 therefore suggests a superposition of both components:

$$h_c = \frac{k}{l} \left(Nu_v^3 + Nu_{nc}^3 \right)^{1/3} \qquad (14)$$

The heat flux dissipated by the water flow at the last experiment is:

$$q_w = c_w \dot{m} (T_{outlet} - T_{inlet}) \qquad (15)$$

with:

$$\dot{m} = \rho_w \cdot \dot{V} \qquad (16)$$

The heat and power fluxes of the different experiments have been calculated, using data from Tables 2 to 7, the characteristic dimensions given the Figures, and using equations (1) to (16). The results are presented in Table 8; the computed values are reasonably fitting to the measurements with maximal deviations of +5.9% to −7.9%.

SUMMARY & DISCUSSION

Fig. 6 shows the thermal response to the different types of PV facades irradiated at 700 W m^{-2} for four hours. Stationary values are reached after 1-2 hours.

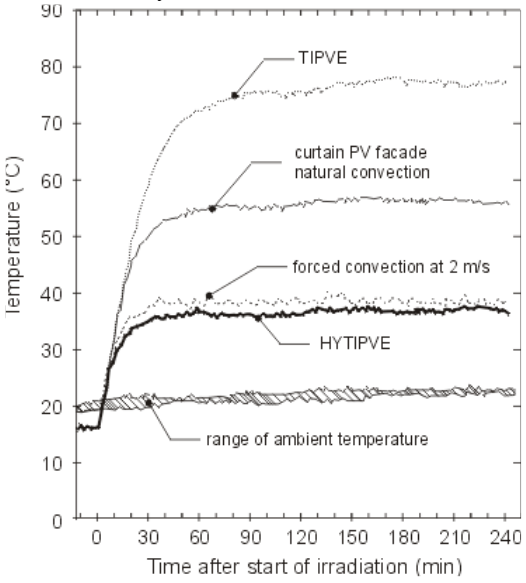

Figure 6. Temperature as a function of time for different types of PV facade elements (G=700Wm^{-2}).

Table 9 offers an overview of the different measures and the consequences on yield and costs:

1. Active ventilation by forced convection of 2 m s^{-1} results in a maximum reduction of operating cell temperatures of 18 K. This leads to an 8% increase in the electrical power output in comparison to conventional PV facades.

2. Thermal insulating PV facade elements (TIPVE) at k = .32 W K^{-1} m^{-1} lead to a temperature increase of 20.7 K, which causes a 9.3% loss of electrical yield (related to conventional PV curtain facades). Depending on the value of the PV-generated electricity in relation to the possible savings in installation costs such a solution may become an attractive option.

3. Hybrid thermal insulating PV facade elements (HYTIPVE), combined with water cooling systems (which may also be used for hot water applications) allow an electrical yield that is 9% higher than for conventional PV-facades.

In order to facilitate further simulation of cell temperatures, efficiencies and energy yields, the model of the thermal process was given. The simulation carried out (see Table 8) showed reasonable small deviations to the measurements and can be used for further investigations of building integration of photovoltaic elements. Energy

consumption of equipment used for ventilation and pumping are not representative. Wachsmann 2000 gives some first results relating pumping power to gain of PV yield by cooling for large PV pumping systems. Economic investigations concerning the invested and operational costs of additional components (as fans, water pumps, insulation, installation and substitutive effects) relating to the yield are given on the way.

ACKNOWLEDGEMENTS

The authors would like to express their sincere thanks to Bodo von Moltke who built the solar simulator, to Leopoldo Bastos who enabled instrumentation to measure air velocity, also to Rodrigo Guido Araújo who built the solar simulator in Rio, and for the support of Solon AG who financed a major part of this project.

Table 6. Properties of air at different temperatures (data by VDI 1994)

Property \ Temperature	20 °C	30 °C	40 °C	50°C *)	60 °C
C_p in kJ $K^{-1}kg^{-1}$	1.007	1.007	1.007	1.008	1.009
k in 10^{-3} W m^{-1} K^{-1}	25.69	26.43	27.16	27.88	28.60
Pr in -	.7148	.7134	.7122	.7111	.7100
β in 10^{-3} K^{-1}	3.421	3.307	3.200	3.104	3.007
ρ in kg m^{-3}	1.188	1.149	1.112	1.079	1.045
ν in 10^{-6} m^2 s^{-1}	15.35	16.30	17.26	18.27	19.27
μ in 10^{6} kg m^{-1} s^{-1}	18.24	18.72	19.20	19.72	20.24

*) values by linear interpolation.

Table 7. Thermal emittances of module and building materials (20°C-80°C)

Material	Emittance ε	References
Aluminium (oxidized)	0.2	VDI 1994
Glass	0.94	VDI 1994
White paint	0.925	VDI 1994
Building surface	0.91	Grigull and Blanke 1989
Wood (pressboard)	0.90	Grigull and Blanke 1989
Back cover of module (PTFE)	0.97	Grigull and Blanke 1989

Table 8. Simulation of heat and power flows for different types of PV facade elements (PVE), calculated according to equations (1) to (15) using data from Tables 2 to 7.

Energy flow	HYTIPVE flow rate 47.7· 10^{-6} m^3/s	PVE ventilated at 2 m/s	conv. PVE - air duct of 150 mm	TIPVE
$\rho_{opt} G$ in W m^{-2}	92.0	92.0	92.0	92.0
P_{PV}/A in W m^{-2}	54.1	53.3	43.8	42.3
q_k in W m^{-2}	4.2	0	0	17.4
Q_{rf} in W m^{-2}	81.4	94.4	219.3	393.2
q_{rb} in W m^{-2}	0	94.4	110.4*)	0
Q_{cf} in W m^{-2}	35.9	164.3	109.7	196.5
Q_{cb} in W m^{-2}	0	164.3	125.2	0
Q_w in W m^{-2}	379.2	0	0	0
Sum of energy flows in W m^{-2}	**646.8**	**662.7**	**700.4**	**741.4**
Relative difference from 700 W m^{-2}	- 7.6%	- 5.3%	+ 0.06%	+ 5.9 %

*) At the conv. PVE wall temperature was set to $T_{aw}=0.5(T_b+T_a)$ for radiation exchange between module back and wall.

Table 9. Measurements of stationary temperatures for different types of PV facade elements (PVE)

	HYTIPVE flow rate $47.7 \cdot 10^{-6}$ m^3/s	PVE ventilated at 2 m/s	conv. PVE - air duct of 150 mm	TIPVE
T_{cell} in °C	36.8	39.6	55.9	77.1
T_a in °C	23.1	24	22.2	22.8
ΔT_{cell} vs. conventional PV façade in K (ref. To T_a=20°C)	19.9	18	0	20.7
Gain of electrical yield	**9.0 %**	**8.1 %**	**0 %**	**-9.3 %**
Relative expenditure related to conv. PV façade (new building)	1.2-1.4	1.1-1.2	1.0	0.8-0.9

REFERENCES

Mitchell, J. W. and W. A. Beckman, „Instructions for IBPSA Manuscripts“, SEL, University of Wisconsin, Madison WI, 1995.

Bendel C., Rudolph U. and M. Viotto. „PV-Experimental-Fassade - Untersuchungsergebnisse und Kostenreduktionspotentiale“. Proceedings 12th Symposium on Photovoltaic Solar Energy, 26-28 February, Staffelstein, Germany, pp. 76-85, 1997.

Bergende T. and L□vvik O. E. (1996) „Model Calculations on a Flat-Plate Solar Heat Collector with Integrated Solar Cells“. Solar Energy **55**, 453-462.

Brinkworth B. J., Cross B. M., Marshall R. H. and Yang H. X. „Thermal Regulation of Photovoltaic Cladding“. Solar Energy **61**, 169-178 (1997).

Crick F.J., Wishaw A., Pearsall N., Hynes K., Shaw M., Young G. and Baker P. „Photovoltaic Ventilated Facade: System Investigation and Characterisation“. Proceedings of the 14th European Photovoltaic Solar Energy Conference World Conference on Photovoltaic Energy Conversion, 30 June-4 July, Barcelona, Spain,, pp. 1914-1917 (1997).

Crick F.J., Wishaw A., Pearsall N., Hynes K., Shaw M., Young G. and Baker P. „PV cladding thermal gains: experimental results from three PV cladding systems investigating the effects on the design on the operational temperature“. In Proceedings of the 2nd World Conference and exhibition on Photovoltaic Energy Conversion, 6-10 July, Vienna, Austria, pp. 2062-2065, (1998).

Churchill S. W. „A Comprehensive Correlating Equation for Laminar, Assisting, Forced and Free Convection“. AIChE **10**, 10-16, (1977).

Emery K., Burdick J., Caiyem Y., Dunlavy D., Field H., Kroposki B. and T. Moriatry T. „Temperature Dependence of Photovoltaic Cells, Modules, and Systems“. Proceedings of the 25th IEEE PV Specialists Conference, May 13-19, Washington DC, USA, pp. 1275-1278 (1996).

Grigull U. and W. Blanke, „Thermo-physikalische Stoffgrößen“. Berlin, Heidelberg New York: Springer, 1989.

Hänel A. and M. S. Imamura, „Improvement of PV Array Performance“. Proceedings of the 11th E.C. Photovoltaic Conference, 12-16 October, Montreux, Switzerland, pp. 1088-1093 (1992).

King D. L. and Eckert P. E. „Characterizing (Rating) the Performance of Large Photovoltaic Arrays for All Operating Conditions“. Proceedings of the 25th IEEE PV Specialists Conference, May 13-19, Washington DC, USA, pp. 1385-1388 (1996).

Krauter S. „Betriebsmodell der optischen, thermischen und elektrischen Parameter von PV-Modulen. Berlin: Verlag Köster, 1993.

Krauter S. and R. Hanitsch „Actual Optical and Thermal Performance of PV Modules. Solar Energy Materials and Solar Cells **41/42**, 557-574 (1996).

Merker G. P. „Konvektive Wärmeüber-tragung“. Berlin, Heidelberg, New York: Springer, 1987.

Nordmann T., Dürr M. and A. Frölich „The 32 kW PV Installation on the Grain Silo of the Stadtmühle CMZ – the First Installation for the Zurich Solar Power Exchange“. Proceedings of the 2nd World Conference and exhibition on Photovoltaic Energy Conversion, 6-10 July, Vienna, Austria, pp. 1983-1986 (1998).

Posansky M. and S. Gnos „Building Integrated Photovoltaic Systems: Examples of realised Hybrid PV-Power Plants with specially conceived PV-Modules for Building Integration“. Proceedings of the 12th E.C. Photovoltaic Conference, 11-14 April. Amsterdam, Netherlands. (1994)

Sandberg M. and Moshfegh B. „Flow and Heat Transfer in the air gap behind photovoltaic panels“.

Renewable and Sustainable Energy Reviews **2**, 287-301 (1998).

VDI „VDI Wärmeatlas“, 7th Ed., Verband Deutscher Ingenieure (Eds), VDI, Düsseldorf, Germany, 1994.

Wachsmann, U., „Extended Use of Photovoltaic Pumping Systems“. Master thesis at UFRJ and TU Berlin (in German), 2000.

Wilshaw A. R., Bates J. R. and N. M. Pearsall. „Photovoltaic Module Operating Temperature Effects“. Proceedings of EuroSun'96, Munich, Germany, pp. 940-944 (1996).

NOMENCLATURE

A	Area (m^2)
AM	Relative Air Mass
c	Specific heat ($J\,kg^{-1}\,K^{-1}$)
d	Depth of air duct (m)
E	Irradiance ($W\,m^{-2}$)
G	Global irradiance ($W\,m^{-2}$)
Gr	Grashof number (-)
g	Standard gravitational acceleration ($9.8067\,m\,s^{-2}$)
h	Heat transfer coefficient ($W\,m^{-2}\,K^{-1}$)
HYTIPVE	Hybrid Thermal Insulating PV facade Element
I	Electrical current (A)
I_{mpp}	Current at Maximum Power Point (A)
I_{sc}	Short circuit current (A)
k	Thermal conductivity ($W\,m^{-1}\,K^{-1}$)
l	characteristic length relevant for heat transfer (m)
m	Mass (kg)
$\dot{m}$	Mass flow ($kg\,s^{-1}$)
MPP	Maximum Power Point
Nu	Nusselt number
P	Electrical power (W)
P_{mpp}	Electrical power at Maximum Power Point (W)
Pr	Prandl number (-)
PV	Photovoltaic
PVE	Photovoltaic Facade Element
Pt 100	Electrical resistor made of Platinum used for temperature measurements (100 Ohms at 0°C)
q	Heat flux ($W\,m^{-2}$)
Ra	Raleigh number (-)
Re	Reynolds number (-)
Si	Silicon
STC	Standard Test Conditions (irradiance of 1000 W m^2, spectrum AM 1.5, and a solar cell temperature of 25°C)
t	Time (s)
T	Temperature (°C, K)
T_{cell}	Solar cell temperature (°C, K)
T_{center}	Backside temperature at the center of a PV module (°C, K)
T_{inlet}	Temperature of water inlet (°C, K)
T_{lower}	Backside temperature at the lower part of the PV module (°C, K)
T_{outlet}	Temperature of water outlet (°C, K)
T_{upper}	Backside temperature at the upper part of the PV module (°C, K)
TC_V	Temperature coefficient of voltage dV/dT ($V\,K^{-1}$)
TC_C	Temperature coefficient of current dC/dT ($A\,K^{-1}$)
TC_P	Temperature coefficient of power dP/dT ($W\,K^{-1}$)
TIPVE	Thermal Insulating PV facade element
v	Air velocity ($m\,s^{-1}$)
V	Voltage (V)
V_{mpp}	Voltage at Maximum Power Point (V)
V_{oc}	Open circuit voltage (V)
$\dot{V}$	Volume flow ($m^3\,s^{-1}$)
WSV 95	German Heat Preserving Edict of 1995 (“Wärmeschutzverordnung”)

Greek letters

β	Thermal expansion coefficient (K^{-1})
ΔT_{cell}	Difference of cell temperature related to reference conditions (K)
η_{PV}	Efficiency of PV conversion (-)
ε	Thermal emittance (-)
λ	Wavelength (m)
ν	Cinematic viscosity ($m^2\,s^{-2}$)
μ	Dynamic viscosity ($kg\,m^{-1}\,s^{-1} = N\,m^{-2}\,s^{-1} = Pa\,s$)
ρ	Density ($kg\,m^{-3}$)
ρ_{op}	Optical reflectance (-)
σ	Stefan Boltzmann constant ($5.67\,10^{-8}$ $W\,m^{-2}\,K^{-4}$)

Subscripts

a	ambient
aw	artificial wall
b	backside
bw	building wall
c	convective
cf	convective front
cb	convective back
f	front
k	conductive
kf	conductive front
kb	conductive back
lam	laminar
nc	natural convection
r	radiative
rb	radiative back
rf	radiative front
tur	turbulent
v	forced convection
w	water